Description of the Giant Monopole Resonance in the Even-A $^{112-124}$Sn Isotopes within the Microscopic Model Including Quasiparticle-Phonon Coupling

A. Avdeenkov,[1,2] F. Grümmer,[1] S. Kamerdzhiev,[1,3] S. Krewald,[1]
E. Litvinova,[4,3] N. Lyutorovich,[1,5] J. Speth,[1] and V. Tselyaev[1,5]

[1]*Institut für Kernphysik, Forschungszentrum Jülich, 52425 Jülich, Germany*
[2]*Skobeltsyn Institute of Nuclear Physics, Moscow State University, 119991 Moscow, Russia*
[3]*Institute of Physics and Power Engineering, 249033 Obninsk, Russia*
[4]*Gesellschaft für Schwerionenforschung mbH, Planckstraße 1, 64291 Darmstadt, Germany*
[5]*Nuclear Physics Department, V. A. Fock Institute of Physics, St. Petersburg State University, 198504 St. Petersburg, Russia*

(Dated: February 22, 2013)

Abstract

We have calculated the strength distributions of the giant monopole resonance in the even-A tin isotopes ($A = 112 - 124$) which were recently measured in inelastic α-scattering. The calculations were performed within two microscopic models: the quasiparticle random phase approximation (QRPA) and the quasiparticle time blocking approximation which is an extension of the QRPA including quasiparticle-phonon coupling. We used a self-consistent calculational scheme based on the HF+BCS approximation. The single-particle continuum was exactly included on the RPA level. The self-consistent mean field and the effective interaction were derived from the Skyrme energy functional. In the calculations, two Skyrme force parametrizations were used. The T5 parametrization with comparatively low value of the incompressibility of infinite nuclear matter ($K_\infty = 202$ MeV) gives theoretical results in good agreement with the experimental data including the resonance widths.

PACS numbers: 21.60.-n, 24.30.Cz, 25.55.Ci, 27.60.+j

I. INTRODUCTION

The investigation of the isoscalar giant monopole resonance (ISGMR), the so-called breathing mode, is one of the fundamental problems of nuclear physics. The energy of the ISGMR enables one to determine parameters characterizing the incompressibility of infinite nuclear matter (INM), in particular, the value of K_∞. These collective resonances can be studied experimentally in inelastic α-scattering at small angles (see, e.g., Ref. [1] and references therein). Theoretical investigations of these states are based mainly on the self-consistent microscopic approaches (see, e.g., Refs. [2, 3, 4, 5, 6, 7, 8, 9, 10, 11, 12]) including, first of all, scaling and constrained Hartree-Fock (HF) models and the random phase approximation (RPA) and on the Landau-Migdal approach that starts with a phenomenological single-particle basis and with the independently parametrized particle-hole zero-range interaction (see, e.g., Refs. [13, 14, 15] and references therein). It is important to note that the incompressibility K_∞ can not be measured directly but it can be deduced theoretically by comparing the experimental energies of the ISGMR with the corresponding calculated values. The most widely used approach is based on the self-consistent HF or RPA calculations of the mean energies of the ISGMR using effective Skyrme or Gogny forces. Because K_∞ can be calculated from the known parameters of the given force, its value is estimated as the one corresponding to the force that gives the best description of the experimental data. The non-relativistic estimates obtained in such a way lead to the value $K_\infty = 210 \pm 30$ MeV (see, e.g., Refs. [2, 4, 5, 6, 7, 8, 9, 10]), though the recent results favor the upper limit of this estimate (see [11, 12]). In the Landau-Migdal approach one obtains K_∞ from the scalar-isoscalar Landau-Migdal parameter f_0. Here K_∞ was always of the order of 240 MeV [13].

Note that within the relativistic mean-field (RMF) theory the INM incompressibility is usually restricted to the interval $K_\infty = 260 \pm 10$ MeV (see, e.g., Ref. [16]) that is considerably higher than the non-relativistic limits. However, recently it was obtained in Ref. [17] that a zero-range (point-coupling) representation of the effective nuclear interactions in the RMF framework leads to the reduction of K_∞ up to the value of 230 MeV.

In the present paper we investigate theoretically the new experimental data [18] on the strength distributions of the ISGMR in the even-A tin isotopes ($A = 112 - 124$). This is the main goal of our work. The calculations are performed within the framework of the recently

developed microscopic model that takes into account the effects of the quasiparticle-phonon coupling (QPC) in addition to the usual correlations included in the conventional RPA.

The paper is organized as follows. In Sec. II the model is described. The particular attention is paid to the dynamical pairing effects which are important to solve the problem of the 0^+ spurious state in the ISGMR calculations in open-shell nuclei. In Sec. III we describe the details of our calculational scheme and present the results and their discussion. Conclusions are drawn in the last section. Appendix A contains auxiliary formulas.

II. THE MODEL

A. General scheme

Two microscopic models were used in our calculations. The first one is the well-known quasiparticle RPA (QRPA). The basic ingredients of this approximation are the nuclear mean field (including the pairing field operator) and the residual particle-hole (ph) interaction. In the self-consistent QRPA these ingredients are related to each other by the consistency condition. The nuclei excitations are treated as superpositions of the two-quasiparticle (2q) configurations. This model is applicable to a wide range of nuclei including open-shell ones as the pairing correlations of nucleons are taken into account. The QRPA reproduces well the centroid energies and total strengths of giant multipole resonances but not their widths. In order to reproduce the total widths of the resonances it is necessary to enlarge the configuration space by adding 4q configurations, i.e. to extend the (Q)RPA. The most successful approaches in this direction are the models which take into account the QPC in addition to the correlations included in the (Q)RPA (see Refs. [15, 19, 20] and references therein).

In the present investigation the QPC contributions are included within the framework of the recently developed quasiparticle time blocking approximation (QTBA) which is an extension of the QRPA in this sense. On the other hand, since in the QTBA the pairing correlations are also included, this model is a generalization of the method of chronological decoupling of diagrams [21] which is a base of the Extended Theory of Finite Fermi Systems [15]. Details of the QTBA model are described in Refs. [22, 23]. The basic equation of our approach (both in the QRPA and in the QTBA) is the equation for the effective response

function $R^{\rm eff}(\omega)$. In the shorthand notations it reads (we will follow notations of Ref. [23])

$$R^{\rm eff}(\omega) = A(\omega) - A(\omega)\,\mathcal{F}\,R^{\rm eff}(\omega) \tag{1}$$

where $A(\omega)$ is a correlated propagator and $\mathcal{F}$ is an amplitude of the effective residual interaction. In the case of the QRPA, $A(\omega)$ reduces to the uncorrelated 2q propagator $\tilde{A}(\omega)$. In the general case including pairing correlations, the amplitude $\mathcal{F}$ can be represented as a sum of two terms

$$\mathcal{F} = \mathcal{F}^{(\rm ph)} + \mathcal{F}^{(\rm pp)} \tag{2}$$

where the amplitude $\mathcal{F}^{(\rm ph)}$ represents interaction in the ph channel and $\mathcal{F}^{(\rm pp)}$ includes contributions of the interaction both in the particle-particle (pp) and in the hole-hole (hh) channels (in the following for brevity we will use the unified term pp channel implying also the hh-channel contributions).

Let us emphasize that the general formulas of the QTBA derived in Ref. [22] are valid both in the self-consistent and in the non-self-consistent approaches. In the present paper, we use self-consistent calculational scheme based on the HF and Bardeen-Cooper-Schrieffer (BCS) approximations (in what follows, we will refer to this scheme as the HF+BCS approximation). The self-consistent mean field and the effective residual interaction were derived from the Skyrme energy functional by means of the known variational equations. In the calculations, the T5 and T6 Skyrme forces (see Ref. [24]) were used.

An important property of these parametrizations is that they produce the nucleon effective mass m^* equal to the bare nucleon mass m. This is a consequence of the fact that the T5 and T6 Skyrme-force parameters are constrained by the relations (see, e.g., [25]):

$$t_2 = -\frac{1}{3}\,t_1\,(5 + 4x_1)\,, \qquad x_2 = -\frac{4 + 5\,x_1}{5 + 4\,x_1}\,. \tag{3}$$

In this case the contribution of the velocity-dependent terms (except for the spin-orbital ones) into the energy functional and the mean field reduces to the derivatives of the nucleon density, i.e. to the simple surface terms. As a consequence, contribution of these terms into the effective interaction derived from such an energy functional also has very simple form. To see this, consider the energy density $\mathcal{H}$ of the Skyrme energy functional $\mathcal{E}$ defined as

$$\mathcal{E} = \int d\boldsymbol{r}\,\mathcal{H}(\boldsymbol{r})\,. \tag{4}$$

In the sufficiently general case it is given, e.g., in Ref. [24]. However, if the equations (3) hold, the energy density acquires the form

$$\begin{aligned}
\mathcal{H} \;=\; & \frac{\hbar^2}{2m}(\tau_n+\tau_p) + \tfrac{1}{2}\,t_0\left[(1+\tfrac{1}{2}\,x_0)\,\rho^2 - (x_0+\tfrac{1}{2})(\rho_n^2+\rho_p^2)\right] \\
+ \; & \tfrac{1}{16}\,t_1\left\{3(1+\tfrac{1}{2}\,x_1)(\boldsymbol{\nabla}\rho)^2 - 3(x_1+\tfrac{1}{2})\left[(\boldsymbol{\nabla}\rho_n)^2+(\boldsymbol{\nabla}\rho_p)^2\right] - x_1\boldsymbol{J}^2 + \boldsymbol{J}_n^2 + \boldsymbol{J}_p^2\right\} \\
- \; & \tfrac{1}{16}\,t_2\left\{(1+\tfrac{1}{2}\,x_2)(\boldsymbol{\nabla}\rho)^2 + (x_2+\tfrac{1}{2})\left[(\boldsymbol{\nabla}\rho_n)^2+(\boldsymbol{\nabla}\rho_p)^2\right] + x_2\boldsymbol{J}^2 + \boldsymbol{J}_n^2 + \boldsymbol{J}_p^2\right\} \\
+ \; & \tfrac{1}{12}\,t_3\left[(1+\tfrac{1}{2}\,x_3)\,\rho^2 - (x_3+\tfrac{1}{2})(\rho_n^2+\rho_p^2)\right]\rho^\alpha \\
+ \; & \tfrac{1}{2}\,W_0\left(\boldsymbol{J}\cdot\boldsymbol{\nabla}\rho + \boldsymbol{J}_n\cdot\boldsymbol{\nabla}\rho_n + \boldsymbol{J}_p\cdot\boldsymbol{\nabla}\rho_p\right) + \mathcal{H}_{\text{Coul}} + \mathcal{H}_{\text{pair}}
\end{aligned} \tag{5}$$

where $\mathcal{H}_{\text{Coul}}$ is the Coulomb energy density including the exchange part in the Slater approximation, i.e.

$$\mathcal{H}_{\text{Coul}}(\boldsymbol{r}) = \frac{e^2}{2}\int d\boldsymbol{r}'\,\frac{\rho_p(\boldsymbol{r})\,\rho_p(\boldsymbol{r}')}{|\boldsymbol{r}-\boldsymbol{r}'|} - \frac{3}{4}\left(\frac{3}{\pi}\right)^{1/3} e^2\,\rho_p^{4/3}(\boldsymbol{r})\,, \tag{6}$$

and $\mathcal{H}_{\text{pair}}$ is the density of the pairing energy. In the applications of the models based on the Skyrme energy functionals it is frequently taken in the simplest form

$$\mathcal{H}_{\text{pair}} = \tfrac{1}{4}\,V_0\left(\varkappa_n^*\varkappa_n + \varkappa_p^*\varkappa_p\right) \tag{7}$$

which was also used in our calculations. In Eqs. (5)–(7), $\rho=\rho_n+\rho_p$, ρ_q, τ_q, and $\boldsymbol{J}_q$ are the normal densities and $\varkappa_q$ is the anomalous local density of the nucleons of the type $q=n,p$ (neutrons or protons). In particular, ρ_q is the local particle density, τ_q is the kinetic-energy density, and $\boldsymbol{J}_q$ is the spin density. They are defined in the usual way (see, e.g., Ref. [26]). In the case of the spherically symmetric nucleus and within the HF+BCS approximation they have the form

$$\rho_q(r) \;=\; \sum_{(1)}\delta_{q_1,q}\,\frac{2j_1+1}{4\pi}\,v_{(1)}^2\,R_{(1)}^2(r)\,, \tag{8}$$

$$\tau_q(r) \;=\; \sum_{(1)}\delta_{q_1,q}\,\frac{2j_1+1}{4\pi}\,v_{(1)}^2\left[(R'_{(1)}(r))^2 + \frac{l_1(l_1+1)}{r^2}R_{(1)}^2(r)\right], \tag{9}$$

$$\boldsymbol{J}_q(r) \;=\; \frac{\boldsymbol{r}}{r^2}\sum_{(1)}\delta_{q_1,q}\,\frac{2j_1+1}{4\pi}\,v_{(1)}^2\left[j_1(j_1+1) - l_1(l_1+1) - \tfrac{3}{4}\right]R_{(1)}^2(r)\,, \tag{10}$$

$$\varkappa_q(r) \;=\; \sum_{(1)}\delta_{q_1,q}\,\frac{2j_1+1}{4\pi}\,u_{(1)}\,v_{(1)}\,R_{(1)}^2(r)\,. \tag{11}$$

Here and in the following we use the notations of Refs. [22, 23] for the single-quasiparticle basis functions in the doubled space $\tilde{\psi}_1$ which are labelled by the composite indices

$1 = \{[1], m_1\}$ where $[1] = \{(1), \eta_1\}$, $(1) = \{q_1, n_1, l_1, j_1\}$, and $\eta_1 = \pm 1$ is the sign of the quasiparticle energy $E_1 = \eta_1 E_{(1)}$. I.e., the symbol (1) stands for the set of the single-particle quantum numbers excepting the projection of the total angular momentum m_1, $R_{(1)}(r)$ is the radial part of the single-particle wave function, $v^2_{(1)}$ is the occupation probability, and $u_{(1)} = \sqrt{1 - v^2_{(1)}}$.

As can be seen from Eqs. (4) and (5), the following equality holds

$$\frac{\delta \mathcal{E}}{\delta \tau_q(\boldsymbol{r})} = \frac{\hbar^2}{2m} = \text{constant}\,. \tag{12}$$

In particular, it means that the equations of motion derived from such an energy functional $\mathcal{E}$ contain the nucleon effective mass $m^*_q(r) = m$. The spin-scalar part of the effective interaction in the ph channel corresponding to $\mathcal{E}$ is determined by the relation

$$\mathcal{F}^{(\mathrm{ph})}_{0,\,qq'}(\boldsymbol{r}, \boldsymbol{r}') = \frac{\delta^2 \mathcal{E}}{\delta \rho_q(\boldsymbol{r})\, \delta \rho_{q'}(\boldsymbol{r}')}\,. \tag{13}$$

This ansatz completely includes velocity-dependent contributions because of Eq. (12). In the explicit form we have

$$\begin{aligned}
\mathcal{F}^{(\mathrm{ph})}_{0,\,nn}(\boldsymbol{r}, \boldsymbol{r}') \;=\; & \Bigg(\tfrac{1}{2}\, t_0\, (1 - x_0) + \tfrac{1}{12}\, t_3 \Bigg\{ (1 + \tfrac{1}{2}\, x_3)\, (1 + \alpha)\, (2 + \alpha)\, \rho^\alpha \\
& - \; (x_3 + \tfrac{1}{2}) \left[2\rho^\alpha + 4\alpha \rho_n \rho^{\alpha - 1} + \alpha(\alpha - 1)(\rho_n^2 + \rho_p^2)\rho^{\alpha - 2} \right] \Bigg\} \Bigg)\, \delta(\boldsymbol{r} - \boldsymbol{r}') \\
& + \; \tfrac{3}{16} \left[t_2\, (1 + x_2) - t_1\, (1 - x_1) \right] \Delta\, \delta(\boldsymbol{r} - \boldsymbol{r}')\,,
\end{aligned} \tag{14}$$

$$\begin{aligned}
\mathcal{F}^{(\mathrm{ph})}_{0,\,np}(\boldsymbol{r}, \boldsymbol{r}') \;=\; & \Bigg(t_0\, (1 + \tfrac{1}{2}\, x_0) + \tfrac{1}{12}\, t_3 \Bigg\{ (1 + \tfrac{1}{2}\, x_3)\, (1 + \alpha)\, (2 + \alpha)\, \rho^\alpha \\
& - \; (x_3 + \tfrac{1}{2})\, \alpha \left[(\alpha + 1)\rho^\alpha - 2(\alpha - 1)\rho_n\, \rho_p\, \rho^{\alpha - 2} \right] \Bigg\} \Bigg)\, \delta(\boldsymbol{r} - \boldsymbol{r}') \\
& + \; \tfrac{1}{8} \left[t_2\, (1 + \tfrac{1}{2} x_2) - 3 t_1\, (1 + \tfrac{1}{2} x_1) \right] \Delta\, \delta(\boldsymbol{r} - \boldsymbol{r}')\,.
\end{aligned} \tag{15}$$

The formulas for the components $\mathcal{F}^{(\mathrm{ph})}_{0,\,pp}$ and $\mathcal{F}^{(\mathrm{ph})}_{0,\,pn}$ are obtained from Eqs. (14) and (15) by replacing indices n by p and p by n and by adding the Coulomb interaction to $\mathcal{F}^{(\mathrm{ph})}_{0,\,pp}$.

Let us note that in addition to the simplicity of the formulas for the effective residual interaction there exist the physical reasons to use the Skyrme forces with $m^* = m$. It is known that for heavy and medium mass nuclei the single-particle spectra obtained in the HF calculations with such Skyrme forces better reproduce the experimental energies as compared with the case of the forces with $m^*/m \sim 0.7$. This results in better description

of the excitations of the even-mass nuclei in the RPA and QRPA. The same is true for the QTBA if the subtraction procedure (see Eq. (19) below and Refs. [22, 23]) is used.

The spin-vector components of the effective interaction are not determined uniquely from Eq. (5) which is valid only for the spin-saturated nuclei. In our calculations these components are taken in the simple form of the Landau-Migdal zero-range force with known parameters C_0, g, and g' (see, e.g., Ref. [23]). However, the spin-vector components of the interaction do not enter equations for the 0^+ excitations.

Note that in the fully self-consistent HF-RPA calculations [27] it was obtained that the spin-orbital and the Coulomb components of the effective residual interaction slightly shift the mean energy of the ISGMR in the opposite directions. This effect is also confirmed by our estimates of the mean energies of the ISGMR based on the constrained HF method described in Ref. [3] (see also [10] for details of our calculational scheme). Namely, in the test calculations for ^{120}Sn we have obtained the following results using T5 Skyrme force and neglecting pairing correlations. The constrained HF method (fully including the spin-orbital and the Coulomb contributions) yields for the mean energy $\sqrt{m_1/m_{-1}}$ the value 15.1 MeV where m_1 and m_{-1} are the energy-weighted moments defined by Eq. (22) below for the infinite energy interval ($E_1 = 0$, $E_2 = \infty$). For the same interval we obtain in the RPA the value 15.4 MeV if we neglect only the spin-orbital contributions in the residual interaction. If we neglect both the spin-orbital and the Coulomb contributions in the RPA interaction we obtain the value 15.0 MeV that differs from the constrained HF result only by 0.1 MeV.

In our QRPA and QTBA calculations, the spin-orbital components of the effective interaction (but not of the mean field) are neglected. For the reasons described above we also neglect the Coulomb contribution into $\mathcal{F}^{(\mathrm{ph})}_{0,\,pp}$. The effective interaction in the pp channel and the gap equation within the HF+BCS approximation are determined by the formulas of Appendix A of Ref. [23] with $\mathcal{F}^{\xi}(r) = \frac{1}{2}V_0$ (see also Appendix A of the present paper).

B. Dynamical pairing effects in QRPA and QTBA

One of the important questions arising in the QRPA and QTBA calculations is the question of completeness of the configuration space. The size of the basis in this space has an impact practically on all the calculated quantities. In particular, configurations with a particle in the continuum are responsible for the formation of the escape widths of the

resonances. The well-known method to include these configurations on the RPA level is the use of the coordinate representation within the Green function formalism (see Ref. [28]). We use this method in our approach as described in Ref. [23]. However, incorporation of the pp-channel contributions in the coordinate representation leads to considerable numerical difficulties. At the same time, the pp-channel contributions (so-called dynamical pairing effects) are very important in the calculations of 0^+ excitations in the open-shell nuclei, first of all because of the problem of the 0^+ spurious state. For this reason we have developed a combined method which is a modification of the so-called (r, λ) representation proposed in Ref. [29] for the QRPA problem. Within this method only the ph channel is treated in the coordinate space, while the dynamical pairing effects are included in the discrete basis representation.

Considering the general case of the QTBA, note that taking into account decomposition (2) one can rewrite Eq. (1) in the form

$$R^{\rm eff}(\omega) = A^{\rm (res+pp)}(\omega) - A^{\rm (res+pp)}(\omega)\, \mathcal{F}^{\rm (ph)}\, R^{\rm eff}(\omega) \tag{16}$$

where propagator $A^{\rm (res+pp)}(\omega)$ is a solution of the equation

$$A^{\rm (res+pp)}(\omega) = A(\omega) - A(\omega)\, \mathcal{F}^{\rm (pp)}\, A^{\rm (res+pp)}(\omega)\,. \tag{17}$$

In the present work we use the version of the QTBA in which the ground state correlations caused by the QPC are neglected. In this case the correlated propagator $A(\omega)$ is defined by the equation

$$A(\omega) = \tilde{A}(\omega) - \tilde{A}(\omega)\, \bar{\Phi}(\omega)\, A(\omega) \tag{18}$$

where $\tilde{A}(\omega)$ is the uncorrelated QRPA propagator,

$$\bar{\Phi}(\omega) = \Phi^{\rm (res)}(\omega) - \Phi^{\rm (res)}(0)\,, \tag{19}$$

and $\Phi^{\rm (res)}(\omega)$ is a resonant part of the interaction amplitude responsible for the QPC in our model (see Refs. [22, 23] for details). Combination of Eqs. (17) and (18) leads to the new equation for $A^{\rm (res+pp)}(\omega)$:

$$A^{\rm (res+pp)}(\omega) = \tilde{A}(\omega) - \tilde{A}(\omega)\big[\bar{\Phi}(\omega) + \mathcal{F}^{\rm (pp)}\big] A^{\rm (res+pp)}(\omega)\,. \tag{20}$$

As a result we obtain that the pp-channel contributions can be included by modification of the equation for the correlated propagator, i.e. by replacing Eq. (18) by Eq. (20). The

modification is reduced to the additional term $\mathcal{F}^{(\mathrm{pp})}$ added to the amplitude $\bar{\Phi}(\omega)$. The respective equations in terms of the reduced matrix elements are drawn in Appendix A. It is worth noting that the QPC in the QTBA is included both in the ph channel and in the pp channel because there is no difference between these channels in the representation of the single-quasiparticle basis functions in the doubled space ($\tilde{\psi}_1$, see Ref. [23]) which is used in Eqs. (17), (18), and (20). This is true both for the system of equations (1), (18) and for the system (16), (20).

Note, however, that in practice Eq. (16) for $R^{\mathrm{eff}}(\omega)$ is solved in the coordinate representation (to take into account the single-particle continuum), while Eq. (20) is solved in the restricted discrete basis representation. This fact greatly simplifies the problem as compared with the initial Eq. (1) in which both the ph-channel contribution and the pp-channel one are included in the coordinate representation. On the other hand, the use of the restricted discrete basis representation for the pp channel is fully consistent with BCS approximation in which the gap equation is solved in the same restricted basis.

The general scheme described above ensures that the energy of the 0^+ spurious state (so-called ghost state) is equal to zero both in the QRPA and in the QTBA. However, there still remains the following problem: in the QTBA the ghost state can be fragmented due to its coupling to the 2q$\otimes$phonon configurations, despite the energy of the dominant ghost state is equal to zero. It can lead to the spurious states at low energies distorting respective strength functions. In particular, these fragmented spurious states will produce non-zero response to the particle-number operator which has to be exactly equal to zero in a correct theory (as, for instance, in the QRPA including pp channel that was proved by Migdal, see [30]). In the present calculations this problem is solved with the help of special projection technique which will be described in a forthcoming publication.

III. CALCULATIONS OF THE GIANT MONOPOLE RESONANCE IN THE TIN ISOTOPES

A. Numerical details

The method described above has been applied to calculate the strength distributions of the isoscalar giant monopole resonance in the even-A tin isotopes ($A = 112-124$) which were

recently measured experimentally with inelastic scattering of α particles (see Ref. [18]). The ground state properties of these nuclei were calculated within HF+BCS approximation using T5 and T6 Skyrme forces with the parameters drawn in Ref. [24] including the pairing-force strength $V_0 = -210$ MeV·fm^3 in Eq. (7). For all tin isotopes under consideration, the pairing window for the neutrons contains 22 states including all the discrete states and one or two quasidiscrete states. The criterion to select quasidiscrete states is described in Ref. [23].

To calculate the strength function of the ISGMR, the equation (1) for the effective response function $R^{\rm eff}(\omega)$ was solved. The strength function $S(E)$ is determined by $R^{\rm eff}(\omega)$ via the formula

$$S(E) = \frac{1}{2\pi} \, {\rm Im} \sum_{1234} (eV^0)^*_{21} \, R^{\rm eff}_{12,34}(E + i\Delta) \, (eV^0)_{43} \qquad (21)$$

where E is an excitation energy, Δ is a smearing parameter, V^0 is an external field, and e is an effective charge operator. In the case of the isoscalar 0^+ excitations the one-body operator eV^0 is proportional to the identity matrices both in the spin and in the isospin indices. Its radial dependence is taken in our calculations in the form $eV^0 = r^2$. The smearing parameter was taken to be equal to 500 keV that approximately corresponds to the experimental resolution for the data presented in Ref. [18].

In the calculation of the QTBA correlated propagator $A(\omega)$ entering Eq. (1), the valence zone for the neutrons coincides with the pairing window. The valence zone for the protons contains 20 states including all the discrete states and several quasidiscrete states as described in Ref. [23]. Let us emphasize that the restricted valence zone is used only in the calculation of the discrete part of the propagator $A(\omega)$ including QPC effects and in the calculation of the phonons (see below). In the ISGMR calculations, the configurations with the particle in the continuum are included completely in the RPA-like part of $A(\omega)$ (see Ref. [23] for details).

The set of phonons in the QTBA calculations included collective modes with values of the spin L in the interval $2 \leqslant L \leqslant 9$ and with natural parity $\pi = (-1)^L$. The phonon characteristics were calculated within the QRPA using configuration space restricted by the valence zone described above. The maximal energy of the phonon was adopted to be equal to the value 10 MeV which is approximately equal to the nucleon separation energy for the given tin isotopes. The second criterion to include the phonon into the phonon space was its reduced transition probability $B(EL)$ which should be more than 10% of the maximal

$B(EL)$ for the given spin. According to these criterions, the total number of phonons included in the QTBA calculations is equal to 21 for ^{112}Sn, 19 for ^{114}Sn, 23 for ^{116}Sn, 26 for ^{118}Sn, 29 for ^{120}Sn, 27 for ^{122}Sn, and 31 for ^{124}Sn.

To describe correctly effects of a fragmentation of the resonances in the QTBA arising due to the QPC it is very important to use the phonon space with the phonon characteristics close to the experimental ones. However, both the T5 and the T6 Skyrme forces do not provide satisfactory description of the experimental energies and transition probabilities within the self-consistent QRPA scheme presented in Section II. For this reason, in the calculation of the phonons (and only in this calculation) we have used the QRPA scheme which is self-consistent only on the mean-field level. More specifically, the mean field was calculated within HF+BCS approximation based on the T5 Skyrme force, while the effective residual interaction was taken in the form of the Landau-Migdal zero-range force with the standard set of the parameters (see, e.g., Ref. [31]), except for the parameter $f_{\rm ex}$. This parameter was adjusted for the each nucleus to reproduce the experimental energies of the 2^+_1 and 3^-_1 levels. As a result, the parameter $f_{\rm ex}$ takes the values in the interval -1.54 ± 0.11 for the phonons with the positive parity and the values in the interval -1.83 ± 0.06 for the phonons with the negative parity.

B. Results and discussion

The results for the ISGMR strength distributions in the even-A $^{112-124}$Sn isotopes are presented in Fig. 1 and in Table I. The energy-weighted moments m_k were determined as

$$m_k = \int_{E_1}^{E_2} E^k S(E)\, dE\,. \tag{22}$$

The energy interval limited by $E_1 = 10.5$ MeV and $E_2 = 20.5$ MeV was taken the same as in Ref. [18]. As can be seen from the Table I, the agreement of the theoretical results with the experimental mean energies is good both in the QRPA and in the QTBA. The fact that the mean energies obtained in the QRPA and in the QTBA are very close to each other is explained by the subtraction procedure used in our calculations (see Eq. (19) and Ref. [23] for the discussion). The main reason of the agreement with the experiment is that in this calculation we used the self-consistent scheme based on the T5 Skyrme-force parametrization with comparatively low value of the incompressibility of INM ($K_\infty = 202$ MeV). The other

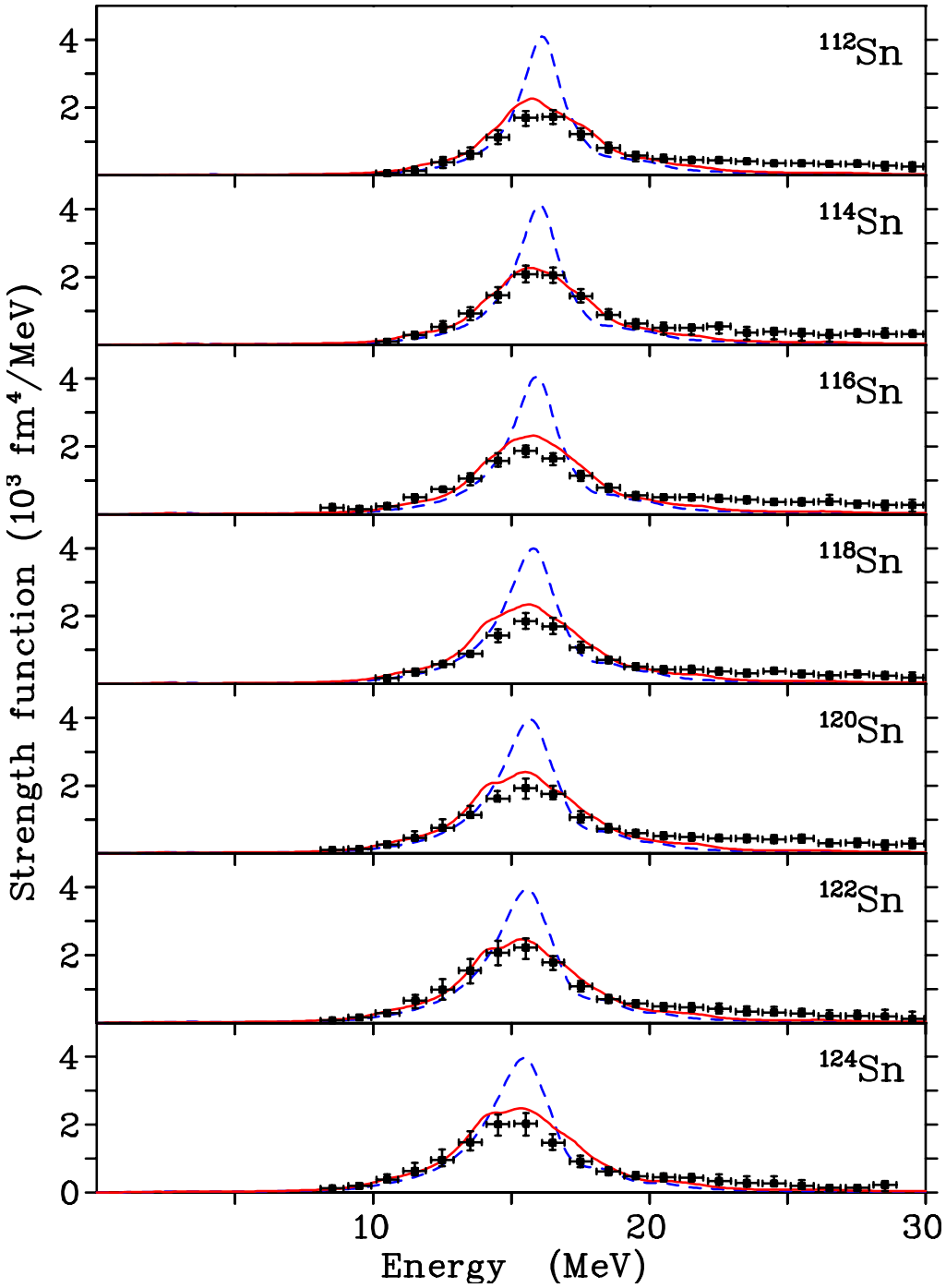

FIG. 1: Isoscalar giant monopole resonance in the even-A $^{112-124}$Sn isotopes calculated within QRPA (dashed line) and QTBA (solid line). The results are obtained within self-consistent HF+BCS approach based on the T5 Skyrme force. The smearing parameter Δ is equal to 500 keV. Experimental data (solid squares) are taken from Ref. [18].

parametrizations with K_∞ around 240 MeV give too large mean energies of the ISGMR in the considered tin isotopes as compared with the experiment.

For comparison, in Table II we draw the QRPA results obtained with the T6 Skyrme force ($K_\infty = 236$ MeV). As can be seen, the T6 mean energies m_1/m_0 are greater than the experimental values for the tin isotopes by more than one MeV. This fact agrees with the results of Ref. [32] where it was obtained that the relativistic RPA calculations based on the force with $K_\infty = 230$ MeV consistently overestimate the centroid energies of the ISGMR in the same tin isotopes.

Note that the value $K_\infty = 202$ MeV corresponding to the T5 Skyrme force lies within the interval 210 ± 30 MeV which was considered for a long time as the non-relativistic estimate for this quantity. The recent results [11, 12] giving K_∞ around 230–240 MeV were obtained on the base of the experimental data in fact only for the one nucleus ^{208}Pb which is doubly magic. However, the question which arises is whether the doubly magic nucleus is the best candidate to determine the value of the INM incompressibility in view of the strong shell effects taking place in this case. On the other hand, by comparing the RPA results for ^{208}Pb shown in the Tables I and II one can see that the T6 Skyrme force with $K_\infty = 236$ MeV nicely reproduces the experimental data for this nucleus ($(m_1/m_0)_{\rm exp} = 14.2 \pm 0.3$ MeV, see [1]), while the T5 force gives the result which is lesser by 1.3 MeV. Thus, the question about the precise value of K_∞ is not resolved within the framework of our approach.

The theoretical values of the ISGMR widths Γ were obtained from the Lorentzian fit of the calculated functions $S(E)$. In contrast to the mean energies, the QRPA and the QTBA give substantially different results for the width. It is well known that the spreading width $\Gamma^\downarrow$ is a considerable part of the total width of the giant resonance. The QRPA does not produce $\Gamma^\downarrow$, while in the QTBA it is formed by the 2q$\otimes$phonon configurations. This is the reason why the QRPA strongly underestimates the experimental values of Γ, while very good agreement is achieved in the QTBA.

To investigate the nature of dependence of the ISGMR mean energies on the neutron excess $(N - Z)$ we calculated the unperturbed $0^+_{\rm IS}$ response substituting the (Q)RPA uncorrelated propagator $\tilde{A}(\omega)$ in Eq. (21) instead of $R^{\rm eff}(\omega)$. This response corresponds to the independent quasiparticle model (IQM). The results are presented in Table III in comparison with the (Q)RPA results obtained in the same energy interval 10–30 MeV. This interval was chosen to exclude contribution of the low-lying strength arising in the IQM response.

TABLE I: Mean energies and widths for the ISGMR strength distributions in the even-A $^{112-124}$Sn isotopes calculated for 10.5–20.5 MeV energy interval. Theoretical results are obtained within self-consistent HF+BCS approach based on the T5 Skyrme force ($K_\infty = 202$ MeV). Experimental values are taken from Ref. [18]. The RPA results for ^{100,132}Sn and ^{208}Pb are drawn for comparison. The values for ^{208}Pb are calculated for 5–25 MeV energy interval.

		$\sqrt{m_1/m_{-1}}$, MeV	m_1/m_0, MeV	$\sqrt{m_3/m_1}$, MeV	Γ, MeV
^{100}Sn	RPA	16.4	16.5	16.7	2.2
	QRPA	16.0	16.1	16.3	1.9
^{112}Sn	QTBA	15.9	16.0	16.4	3.9
	Experiment	16.1 ± 0.1	16.2 ± 0.1	16.7 ± 0.2	4.0 ± 0.4
	QRPA	15.9	15.9	16.2	2.0
^{114}Sn	QTBA	15.7	15.9	16.3	3.9
	Experiment	15.9 ± 0.1	16.1 ± 0.1	16.5 ± 0.2	4.1 ± 0.4
	QRPA	15.7	15.8	16.1	2.1
^{116}Sn	QTBA	15.6	15.7	16.1	4.0
	Experiment	15.7 ± 0.1	15.8 ± 0.1	16.3 ± 0.2	4.1 ± 0.3
	QRPA	15.6	15.7	16.0	2.3
^{118}Sn	QTBA	15.5	15.6	16.0	4.2
	Experiment	15.6 ± 0.1	15.8 ± 0.1	16.3 ± 0.1	4.3 ± 0.4
	QRPA	15.4	15.5	15.8	2.4
^{120}Sn	QTBA	15.3	15.5	15.9	4.3
	Experiment	15.5 ± 0.1	15.7 ± 0.1	16.2 ± 0.2	4.9 ± 0.5
	QRPA	15.3	15.4	15.7	2.5
^{122}Sn	QTBA	15.2	15.4	15.8	4.4
	Experiment	15.2 ± 0.1	15.4 ± 0.1	15.9 ± 0.2	4.4 ± 0.4
	QRPA	15.2	15.3	15.6	2.6
^{124}Sn	QTBA	15.1	15.3	15.7	4.4
	Experiment	15.1 ± 0.1	15.3 ± 0.1	15.8 ± 0.1	4.5 ± 0.5
^{132}Sn	RPA	14.8	14.9	15.2	2.7
^{208}Pb	RPA	12.7	12.9	13.4	1.8

TABLE II: Mean energies and widths for the ISGMR strength distributions in the even-A $^{112-124}$Sn isotopes calculated within the QRPA for 10.5–20.5 MeV energy interval. The calculations were performed within self-consistent HF+BCS approach based on the T6 Skyrme force (K_∞ = 236 MeV). The RPA results for ^{100,132}Sn and ^{208}Pb are also shown. The values for ^{208}Pb are calculated for 5–25 MeV energy interval.

	$\sqrt{m_1/m_{-1}}$, MeV	m_1/m_0, MeV	$\sqrt{m_3/m_1}$, MeV	Γ, MeV
^{100}Sn	17.4	17.5	17.8	2.4
^{112}Sn	17.1	17.2	17.4	2.2
^{114}Sn	17.0	17.1	17.3	2.3
^{116}Sn	16.8	16.9	17.2	2.4
^{118}Sn	16.7	16.8	17.1	2.5
^{120}Sn	16.6	16.7	17.0	2.7
^{122}Sn	16.5	16.6	16.9	2.8
^{124}Sn	16.3	16.5	16.8	3.0
^{132}Sn	16.0	16.1	16.5	3.2
^{208}Pb	13.9	14.1	14.7	2.0

As can be seen from Table III, the $(N-Z)$ dependence of the (Q)RPA mean energies practically follows the dependence of the IQM energies. In particular, the difference between the m_1/m_0 values for ^{112}Sn and ^{124}Sn in the QRPA is equal to 0.9 MeV and the same difference is obtained in the IQM calculation. Since the poles of the uncorrelated propagator $\tilde{A}(\omega)$ are equal to the sums of the quasiparticle energies $E_{(1)} + E_{(2)}$ [see Eq. (A3)], this result means that the $(N-Z)$ dependence of the ISGMR mean energies is mainly determined by the level density of the single-quasiparticle spectrum. Including the residual interaction in the (Q)RPA, we obtain the following redistribution of the isoscalar monopole strength: the low-lying part of the strength disappears, while the mean energy of the high-lying states (which form the ISGMR) is reduced by approximately two MeV.

In Table III, we also include the ISGMR mean energies obtained within the RPA for ^{120}Sn nucleus. In this calculation, the pairing correlations are neglected both in the mean field and in the residual interaction. Respective strength function is shown in Fig. 2 in comparison with the IQM and QRPA strength functions. These results demonstrate that the influence

TABLE III: Mean energies for the $0^+_{\rm IS}$ strength distributions in the even-A $^{100,112-124,132}$Sn isotopes calculated for 10–30 MeV energy interval within self-consistent HF+BCS approach based on the T5 Skyrme force. See text for details.

		$\sqrt{m_1/m_{-1}}$, MeV	m_1/m_0, MeV	$\sqrt{m_3/m_1}$, MeV
^{100}Sn	IQM	19.1	19.3	19.9
	RPA	16.8	17.0	17.6
^{112}Sn	IQM	18.5	18.7	19.4
	QRPA	16.4	16.5	17.1
^{114}Sn	IQM	18.3	18.5	19.3
	QRPA	16.2	16.4	17.0
^{116}Sn	IQM	18.1	18.4	19.1
	QRPA	16.0	16.2	16.8
^{118}Sn	IQM	17.9	18.2	19.0
	QRPA	15.9	16.0	16.7
	IQM	17.8	18.1	18.9
^{120}Sn	QRPA	15.7	15.9	16.5
	RPA	15.2	15.4	16.0
^{122}Sn	IQM	17.6	17.9	18.7
	QRPA	15.6	15.7	16.4
^{124}Sn	IQM	17.5	17.8	18.6
	QRPA	15.4	15.6	16.3
^{132}Sn	IQM	17.1	17.4	18.2
	RPA	15.0	15.2	15.8

of the pairing correlations on the ISGMR mean energies is appreciable. In the QRPA, where the pairing correlations are included, the mean energies increase by 0.5 MeV as compared with the RPA. By comparing the results obtained with the T5 and T6 Skyrme forces, one can see that this increase is substantial for determining the INM incompressibility.

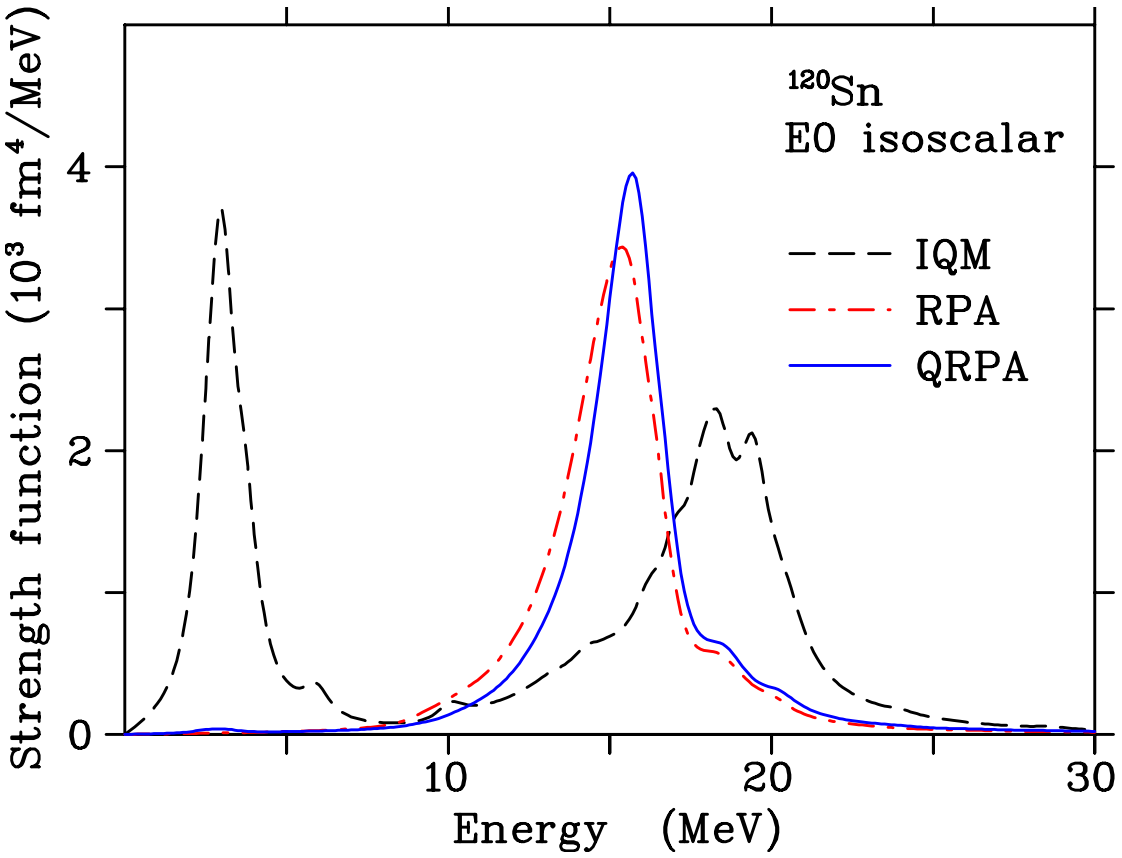

FIG. 2: Isoscalar E0 response in ^{120}Sn calculated within the independent quasiparticle model (IQM, dashed line), RPA (dashed-dotted line), and QRPA (solid line), making use of the T5 Skyrme force. See text for details. The smearing parameter Δ is equal to 500 keV.

IV. CONCLUSIONS

In the paper the results of the theoretical analysis of the ISGMR strength distributions in the even-A $^{112-124}$Sn isotopes are presented. The calculations were performed within two microscopic models: the quasiparticle random phase approximation (QRPA) and the quasiparticle time blocking approximation (QTBA) which is an extension of the QRPA including quasiparticle-phonon coupling. We used self-consistent calculational scheme based on the HF+BCS approximation. The self-consistent mean field and the effective interaction were derived from the Skyrme energy functional. In the calculations, two Skyrme force parametrizations were used. The T5 parametrization with comparatively low value of the incompressibility of infinite nuclear matter (K_∞ = 202 MeV) allowed us to achieve good agreement with the experimental data for tin isotopes within the QTBA including resonance

widths. However, this parametrization fails to reproduce the experimental ISGMR energy for the ^{208}Pb nucleus which is usually used in the fit of the Skyrme force parameters. On the other hand, the T6 Skyrme force with $K_\infty = 236$ MeV nicely reproduces the ISGMR energy for ^{208}Pb but overestimates the energies for $^{112-124}$Sn isotopes by more than one MeV. On the whole, these results do not allow us to decrease the ambiguity in the value of K_∞ as compared with the previous known estimates. Note, however, that the main goal of our work is not to solve the problem of the nuclear matter incompressibility but to find under which conditions one can obtain reasonable description of the experimental data for the considered tin isotopes within the framework of the self-consistent approach including correlations beyond the QRPA.

Acknowledgments

The work was supported by Deutsche Forschungsgemeinschaft under the grant No. 436 RUS 113/806/0-1 and by the Russian Foundation for Basic Research under the grant No. 05-02-04005-DFG_a. V. T. thanks the Institut für Kernphysik at the Forschungszentrum Jülich for hospitality during the completion of this work.

APPENDIX A: MODIFICATION OF THE QTBA EQUATIONS INCLUDING CONTRIBUTION OF THE PARTICLE-PARTICLE CHANNEL IN TERMS OF THE REDUCED MATRIX ELEMENTS

In the detailed form using the notations of Ref. [23] for the reduced matrix elements, our method to include pp-channel contribution in the QTBA equations consists in the following. In Eq. (33) of Ref. [23] only ph channel is kept, but in Eq. (42) for $A^{J\,(\mathrm{ph,ph})\,LS,L'S'}_{[12,34]}(\omega)$ the matrix element $A^{J}_{[12,34]}(\omega)$ is replaced by $A^{J\,(\mathrm{res+pp})}_{[12,34]}(\omega)$ where

$$A^{J\,(\mathrm{res+pp})}_{[12,34]}(\omega) = \delta_{\eta_1,-\eta_2}\,\delta_{\eta_3,-\eta_4}\,A^{J\,(\mathrm{res+pp})}_{(12)\eta_1,\,(34)\eta_3}(\omega)\,. \tag{A1}$$

Propagator $A^{J\,(\mathrm{res+pp})}_{(12)\eta,\,(34)\eta'}(\omega)$ is a solution of the equation

$$A^{J\,(\mathrm{res+pp})}_{(12)\eta,\,(34)\eta'}(\omega) = \tilde{A}^{J}_{(12)\eta,\,(34)\eta'}(\omega) + \sum_{\eta''}\sum_{(56)}\theta_{(65)}\,\bar{\mathcal{K}}^{J\,(\mathrm{res+pp})}_{(12)\eta,\,(56)\eta''}(\omega)\,A^{J\,(\mathrm{res+pp})}_{(56)\eta'',\,(34)\eta'}(\omega)\,, \tag{A2}$$

where

$$\tilde{A}^{J}_{(12)\eta,\,(34)\eta'}(\omega) = -\frac{\eta\,\delta_{\eta,\eta'}\left[\delta_{(13)}\,\delta_{(24)} + (-1)^{J+l_1-l_2+j_1-j_2}\,\delta_{(14)}\,\delta_{(23)}\right]}{2\left(\omega - \eta\left[E_{(1)} + E_{(2)}\right]\right)}\,, \tag{A3}$$

$$\bar{\mathcal{K}}^{J\,(\mathrm{res+pp})}_{(12)\eta,\,(34)\eta'}(\omega) = \frac{\eta\left[\bar{\Phi}^{J\,(\mathrm{res+pp})}_{(12)\eta,\,(34)\eta'}(\omega) + (-1)^{J+l_1-l_2+j_1-j_2}\,\bar{\Phi}^{J\,(\mathrm{res+pp})}_{(21)\eta,\,(34)\eta'}(\omega)\right]}{\omega - \eta\left[E_{(1)} + E_{(2)}\right]}\,, \tag{A4}$$

$$\bar{\Phi}^{J\,(\mathrm{res+pp})}_{(12)\eta,\,(34)\eta'}(\omega) = \sum_{\eta_1\eta_2\eta_3\eta_4} \delta_{\eta_1,\,\eta}\,\delta_{\eta_2,\,-\eta}\,\delta_{\eta_3,\,\eta'}\,\delta_{\eta_4,\,-\eta'}\,\bar{\Phi}^{J\,(\mathrm{res+pp})}_{[12,34]}(\omega)\,, \tag{A5}$$

$$\bar{\Phi}^{J\,(\mathrm{res+pp})}_{[12,34]}(\omega) = \Phi^{J\,(\mathrm{res})}_{[12,34]}(\omega) - \Phi^{J\,(\mathrm{res})}_{[12,34]}(0) + \mathcal{F}^{J(\mathrm{pp})}_{[12,34]}\,. \tag{A6}$$

The order-bounding factors $\theta_{(21)}$ in Eq. (A2) are defined as follows: $\theta_{(21)} = 1$ if the ordinal number of the state (1) is lesser than the number of (2) $[(1) < (2)]$, $\theta_{(21)} = \frac{1}{2}$ if $(1) = (2)$, $\theta_{(21)} = 0$ if $(1) > (2)$. The interaction amplitude $\Phi^{J\,(\mathrm{res})}_{[12,34]}(\omega)$ responsible for the QPC is defined by Eq. (B14) of Ref. [23]. Introducing the notation

$$\mathcal{F}^{J(\mathrm{pp})}_{(12)\eta,\,(34)\eta'} = \sum_{\eta_1\eta_2\eta_3\eta_4} \delta_{\eta_1,\,\eta}\,\delta_{\eta_2,\,-\eta}\,\delta_{\eta_3,\,\eta'}\,\delta_{\eta_4,\,-\eta'}\,\mathcal{F}^{J(\mathrm{pp})}_{[12,34]} \tag{A7}$$

and using Eqs. (C2)–(C4) of Ref. [23] we obtain the following ansatz for this quantity

$$\begin{aligned}
\mathcal{F}^{J(\mathrm{pp})}_{(12)\eta,\,(34)\eta'} &= \delta_{q_1,\,q_2}\,\delta_{q_3,\,q_4}\,\delta_{q_1,\,q_3}\,\frac{1}{2J+1}\langle j_2 l_2||\,T_{JJ\,0}\,||j_1 l_1\rangle\langle j_4 l_4||\,T_{JJ\,0}\,||j_3 l_3\rangle \\
&\times\left[\delta_{\eta,\eta'}\,(u_{(1)}u_{(2)}u_{(3)}u_{(4)} + v_{(1)}v_{(2)}v_{(3)}v_{(4)}) - \delta_{\eta,-\eta'}\,(u_{(1)}u_{(2)}v_{(3)}v_{(4)} + v_{(1)}v_{(2)}u_{(3)}u_{(4)})\right] \\
&\times\int_0^\infty dr\,r^2\,R_{(1)}(r)\,R_{(2)}(r)\,R_{(3)}(r)\,R_{(4)}(r)\,\mathcal{F}^{\xi}(r)\,.
\end{aligned} \tag{A8}$$

Note that the value of $\mathcal{F}^{J(\mathrm{pp})}_{(12)\eta,\,(34)\eta'}$ in Eq. (A8) of the present paper differs from the corresponding value derived from Eqs. (C2) and (C3) of Ref. [23] by a factor $\frac{1}{2}$ due to the shorthand summation used in Eq. (C1) $[(3) \leqslant (4)]$. In addition, in the case $J = 0$ one should set: $\mathcal{F}^{J(\mathrm{pp})}_{(12)\eta,\,(34)\eta'} = \delta_{(12)}\,\delta_{(34)}\,\mathcal{F}^{J(\mathrm{pp})}_{(11)\eta,\,(33)\eta'}$ in order to obtain consistency with the gap equation (A25) of Ref. [23] written in the diagonal approximation. Note that this method is applicable both in the QTBA and in the QRPA. In the latter case the amplitudes $\Phi^{J(\mathrm{res})}$ in Eq. (A6) are set to be equal to zero.

[1] D. H. Youngblood, H. L. Clark, and Y.-W. Lui, Phys. Rev. Lett. **82**, 691 (1999).

[2] J. P. Blaizot, D. Gogny, and B. Grammaticos, Nucl. Phys. **A265**, 315 (1976).

[3] O. Bohigas, A. M. Lane, and J. Martorell, Phys. Rep. **51**, 267 (1979).

[4] J. P. Blaizot, Phys. Rep. **64**, 171 (1980).

[5] J. Treiner, H. Krivine, O. Bohigas, and J. Martorell, Nucl. Phys. **A371**, 253 (1981).

[6] J. P. Blaizot, J. F. Berger, J. Dechargé, and M. Girod, Nucl. Phys. **A591**, 435 (1995).

[7] M. Farine, J. M. Pearson, and F. Tondeur, Nucl. Phys. **A615**, 135 (1997).

[8] Nguyen Van Giai, P. F. Bortignon, G. Colò, Z.-M. Ma, and M. R. Quaglia, Nucl. Phys. **A687**, 44c (2001).

[9] S. K. Patra, X. Viñas, M. Centelles, and M. Del Estal, Nucl. Phys. **A703**, 240 (2002).

[10] V. B. Soubbotin, V. I. Tselyaev, and X. Viñas, Phys. Rev. C **69**, 064312 (2004).

[11] G. Colò, N. Van Giai, J. Meyer, K. Bennaceur, and P. Bonche, Phys. Rev. C **70** 024307 (2004).

[12] H. Sagawa, S. Yoshida, G.-M. Zeng, J.-Z. Gu, and X.-Z. Zhang, Phys. Rev. C **76** 034327 (2007).

[13] P. Ring and J. Speth, Nucl. Phys. **A235**, 315 (1974).

[14] J. Wambach, V. A. Madsen, G. A. Rinker, and J. Speth, Phys. Rev. Lett. **39**, 1443 (1977).

[15] S. Kamerdzhiev, J. Speth, and G. Tertychny, Phys. Rep. **393**, 1 (2004).

[16] D. Vretenar, T. Nikšić, and P. Ring, Phys. Rev. C **68**, 024310 (2003).

[17] T. Nikšić, D. Vretenar, G. A. Lalazissis, and P. Ring, Phys. Rev. C **77**, 034302 (2008).

[18] T. Li, U. Garg, Y. Liu et al., Phys. Rev. Lett. **99**, 162503 (2007).

[19] V. G. Soloviev, *Theory of Atomic Nuclei: Quasiparticles and Phonons* (Institute of Physics, Bristol and Philadelphia, USA, 1992).

[20] P. F. Bortignon and R. A. Broglia, Nucl. Phys. **A371**, 405 (1981).

[21] V. I. Tselyaev, Yad. Fiz. **50**, 1252 (1989) [Sov. J. Nucl. Phys. **50**, 780 (1989)].

[22] V. I. Tselyaev, Phys. Rev. C **75**, 024306 (2007).

[23] E. V. Litvinova and V. I. Tselyaev, Phys. Rev. C **75**, 054318 (2007).

[24] F. Tondeur, M. Brack, M. Farine, and J. M. Pearson, Nucl. Phys. **A420**, 297 (1984).

[25] Y. Aboussir, J. M. Pearson, A. K. Dutta, and F. Tondeur, Nucl. Phys. **A549**, 155 (1992).

[26] S. Krewald, V. B. Soubbotin, V. I. Tselyaev, and X. Viñas, Phys. Rev. C **74**, 064310 (2006).

[27] T. Sil, S. Shlomo, B. K. Agrawal, and P.-G. Reinhard, Phys. Rev. C **73**, 034316 (2006).

[28] S. Shlomo and G. Bertsch, Nucl. Phys. **A243**, 507 (1975).

[29] A. P. Platonov and E. E. Saperstein, Nucl. Phys. **A486**, 63 (1988).

[30] A. B. Migdal, *Theory of Finite Fermi Systems and Applications to Atomic Nuclei* (Interscience, New York, 1967).

[31] S. Kamerdzhiev, R. J. Liotta, E. Litvinova, and V. Tselyaev, Phys. Rev. C **58**, 172 (1998).

[32] J. Piekarewicz, Phys. Rev. C **76**, 031301(R) (2007).